The Capacity of Avalanche Photodiode-Detected Pulse Position Modulation

Jon Hamkins and Juan Ceniceros

Jet Propulsion Laboratory, California Institute of Technology
4800 Oak Grove Drive, Pasadena, CA 91109-8099
{hamkins,juan.ceniceros}@jpl.nasa.gov

ABSTRACT

The capacity is determined for an optical channel employing Pulse Position Modulation (PPM) and an Avalanche PhotoDiode (APD) detector. This channel is different from the usual optical channel in that the detector output is characterized by a Webb-plus-Gaussian distribution, not a Poisson distribution. The capacity is expressed as a function of the PPM order, slot width, laser dead time, average number of incident signal and background photons received, and APD parameters. Based on a system using a laser and detector proposed for X2000 second delivery, numerical results provide upper bounds on the data rate and level of background noise that the channel can support while operating at a given BER. For the particular case studied, the capacity-maximizing PPM order is near 2048 for nighttime reception and 16 for daytime reception. Reed-Solomon codes can handle background levels 2.3 to 7.6 dB below the ultimate level that can be handled by codes operating at the Shannon limit.

Keywords: Capacity, pulse position modulation, avalanche photodiode detector, Reed-Solomon, Webb statistics

1. INTRODUCTION

The capacity of a channel is the highest data rate it can reliably support. Whenever the data rate is less than the capacity of the channel, there exists an error-correcting code for the channel that has an output probability of error as small as desired, and conversely, whenever the data rate is more than the capacity the probability of error is bounded away from zero.

The capacity of the optical channel depends on many factors, including the modulation scheme, laser, transmission medium, photodetector, and preamplifier. Unlike the bandlimited additive white Gaussian noise (AWGN) channel in which all performance-influencing factors are relevant to the channel capacity only in how they affect the bandwidth and signal-to-noise ratio, there is not a method to simplify the formulation of the capacity of the optical channel to so few variables. For example, the capacity depends separately on the signal and background light levels, not simply their ratio. In this paper, the functional dependence of the capacity is distilled to the following six major parameters: (1) the PPM order M, (2) the laser pulse width T_s, (3) the necessary dead time between pulses T_d, (4) the average number of signal photons per pulse incident on the detector $\bar{n}_s$, (5) the average number of background photons per slot incident on the detector $\bar{n}_b$, and (6) the detector itself. These parameters are represented by the vector $(M, \bar{n}_s, \bar{n}_b, T_s, T_d, \text{detector})$, and we will write the capacity as $C = C(M, \bar{n}_s, \bar{n}_b, T_s, T_d, \text{detector})$. For an APD detector, the parameters used are the quantum efficiency η, the ionization ratio k_{eff}, noise temperature T, load resistance R, noise equivalent one-sided bandwidth B, bulk leakage current I_b, and surface leakage current I_s. Not explicitly included in the functional description of the capacity is the modulation extinction ratio α_{er} of the laser, which we fix at 10^6 throughout the paper. A description of these parameters is contained in [4, 14].

Numerical results in the paper are based on a system using components currently available and suggested by X2000 2nd delivery for a Mars-type mission. This includes a 1064nm pulsed Q-switched Neodymium-doped Yttrium Aluminum Garnet (Nd:YAG) laser, a super low k_{eff} (SLiK) APD detector made by EG&G, and a transimpedance pre-amplifier.

Future improvements made in lasers and detectors can be evaluated with the methods outlined in this paper. The increase in capacity can be projected by re-evaluating the equations with new $(M, \bar{n}_s, \bar{n}_b, T_s, T_d, \text{detector})$ parameters. We are undertaking this activity for a future paper.

In the following section, the optical channel is described and the notation used in this paper is given. We also discuss the various units in which capacity may be expressed. Section 3 gives the analytic capacity results, including derivations of the capacity of PPM, the probability of uncoded symbol error for the APD and ideal photon counting detectors, and implications of the converse of Shannon's capacity theorem. In Section 4 we give the numerical capacity results, and in Section 5 we state conclusions and discuss future research needed in this area.

The work described was funded by the TMOD Technology Program and performed at the Jet Propulsion Laboratory, California Institute of Technology under contract with the National Aeronautics and Space Administration.

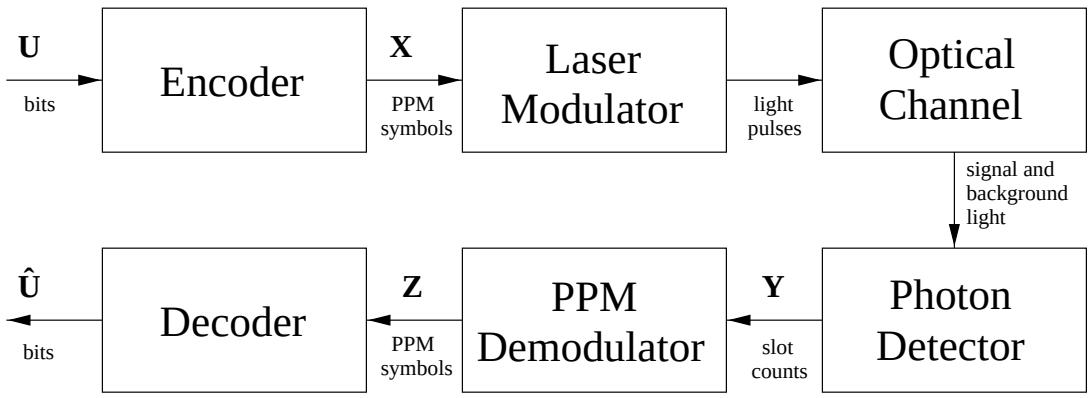

Figure 1. An optical communications system.

2. PRELIMINARIES

2.1. Channel description and notation

2.1.1. Encoder, laser modulator, optical channel

This paper concerns the communications system shown in Fig. 1. The information bits $\mathbf{U} = (U_1, \ldots, U_k)$ are i.i.d. binary random variables assumed to take on the values 0 and 1 with equal probability. The vector $\mathbf{U}$ is encoded to $\mathbf{X} = (X_1, \ldots, X_n)$, a vector of n M-PPM symbols. Each M-PPM symbol is a number in $\{0, \ldots, M-1\}$ (or equivalently, a block of $\log_2 M$ bits, if M is a power of two). There is one signaling slot, and $M-1$ nonsignaling slots for each M-PPM symbol. The symbol indicates to the modulator in which of the M time slots of length T_s to pulse the transmitting laser. Between each M-PPM symbol, the laser requires dead time T_d to recharge and ready itself for sending another pulse. The laser is coupled to a telescope and pulses are transmitted through the optical channel to the receiving telescope, where background light also enters. In Fig. 1, the transmitting telescope, free space, background light, and receiving telescope are grouped under the term "Optical Channel," whose output consists of photons that enter the detector.

2.1.2. Detector

At the receiver, light is focussed on the photodetector, which for this paper we restrict to an APD detector. The detector integrates over slot times to produce $\mathbf{Y} = (\mathbf{Y}_1, \ldots, \mathbf{Y}_n)$, where $\mathbf{Y}_i = (y_{i,1}, \ldots, y_{i,M})$ are the M soft outputs for the ith M-PPM symbol, $1 \leq i \leq n$. The number of photons incident on a detector from an incident optical field of known intensity is a Poisson distributed random variable [4]. The number of photons absorbed by the detector is equal to the number of photons incident times the quantum efficiency η of the detector. The secondary electrons at the output of the detector have a more complicated probability distribution [3, 13, 20]. In this paper, for simplicity we assume perfect timing synchronization and no inter-slot interference, which implies that the number of absorbed photons in each slot is independent of the number of photons absorbed in all other slots. Recent work has developed a method to combat inter-slot interference, assuming Gaussian pulse shapes, by using trellis-coded modulation [10, 17].

2.1.3. PPM demodulator, decoder

Typically, the individual slot statistics at the output of the detector are not available to the decoder.* Instead, for $1 \leq i \leq n$, a PPM demodulator uses the M slot statistics of $\mathbf{Y}_i$ to make an M-PPM symbol decision $Z_i \in \{0, \ldots, M-1\}$ by choosing the slot within each symbol that maximizes the number of detected photons, or in case of a tie, by randomly choosing a slot among those with the maximum statistic. It has recently been proven that this is the maximum likelihood rule for PPM detection when the statistics are governed by the sum of a Webb and Gaussian deviates [19]. Perhaps surprisingly, the maximum likelihood rule becomes more complicated than "pick the largest" when the detector output is approximated by a Gaussian distribution, in which a nonsignaling slot has mean μ_b and variance σ_b^2 and a signaling slot has mean $\mu_b + \mu_s$ and variance $\sigma_b^2 + \sigma_s^2$. We avoid this problem by not using the Gaussian approximations.

*If individual slot statistics are available to the decoder, then the capacity will be higher.

2.2. The units of capacity

This paper expresses the channel capacity in bits per second because ultimately the system designer wants to know how much data can be pumped through the channel how quickly using the given power available. The laser properties, optics efficiency, pointing accuracy, and space and atmospheric losses all affect C, but only through their influence on $\bar{n}_s$, $\bar{n}_b$, T_s, and T_d. Hence we express the capacity as a function of the following parameters:

$$C = C(M, \bar{n}_s, \bar{n}_b, T_s, T_d, \text{detector}).$$

The units in which C is expressed affect the parameter values which maximize C. This fact, which might seem surprising at first, implies that work on maximizing photon efficiency (e.g., [2,5,7,11,12]) does not necessarily help determine the maximum data rate possible on the channel.

2.2.1. Bits per photon or bits per channel use

A channel capacity of C bits per channel use can be restated as $C/\bar{n}_s$ bits per signal photon, C/M bits per PPM slot (neglecting the dead time), and $C/(MT_s + T_d)$ bits per second. The capacity in bits per photon or bits per channel use is not bounded for noiseless PPM, if perfect timing is assumed [16]. (Other practical constraints bound it [11, 12].) Intuitively, the reason is that by choosing increasing values of M and keeping the slot duration fixed, the statistics governing the number of photons detected in the signal slot remain the same, but the number of bits per symbol increases as $\log_2 M$. Thus, the capacity in bits per photon (or bits per channel use) increases as $\log_2 M$, an unbounded number as M increases.

This unbounded capacity in bits/photon is not particularly useful, however, because it necessitates a low data rate and wasted power. Lasers on a spacecraft can have power allocated to them on a continual basis, at least within the intervals of time set aside for transmission to earth. This power is used primarily to charge the laser after it has fired a pulse. If the laser waits an extensive period of time between pulse firings, that power is being wasted. From an information theoretical standpoint, the waste can be quantified by the lost entropy of the signal. The information content of a set of signaling slots (ones) and nonsignaling slots (zeroes) decreases as their probabilities are made more disparate. An increasing M means that the information content per slot (or per unit time) is decreasing, because $M-1$ out of M of the slots contain zeroes.

2.2.2. Bits per second

Instead of using an enormous value of M and transmitting one symbol, we would be better off transmitting two $(M/2)$-PPM symbols in the same amount of time (assuming $M >> T_d/T_s$), because there is a potential for $2\log_2(M/2)$ bits received, as opposed to only $\log_2 M$ bits. Neglecting dead time, the capacity of the errorless channel is $\log_2 M/M$ bits per slot, which is maximized when $M = 3$. (The noninteger maximum occurs when $M = e$.)

The optimum value of M may be much higher than three when the required dead time is taken into account. On an error-free channel using M-PPM, a slot time of T_s and a laser dead time of T_d, the capacity in bits per second is

$$C = \frac{\log_2 M}{MT_s + T_d} \quad \text{bits/second.}$$

M may be chosen to maximize this equation. For the laser used in this paper, $T_s = 3.125 \times 10^{-8}$ seconds and $T_d = 4.32 \times 10^{-4}$ seconds, and an errorless channel capacity is optimized when $M = 2082$. For channels that produce errors, more complicated expressions of capacity result [6], and a different optimal value of M emerges.

3. ANALYTIC RESULTS

In Section 3.1, we derive the capacity of APD-detected PPM, in terms of the PPM order M and the probability of correct uncoded M-PPM symbol detection. A detailed summary of how to compute this probability is then given. In Section 3.2 we use the converse to Shannon's capacity theorem to derive bounds on performance.

3.1. Capacity of APD-detected PPM

3.1.1. Capacity as a function of correct PPM symbol detection

The capacity of the communications system in Fig. 1 is the maximum mutual information between the input and output,

$$C \triangleq \max_{p(\mathbf{X})} I(\mathbf{U};\hat{\mathbf{U}}) = \max_{p(\mathbf{X})} H(\hat{\mathbf{U}}) - H(\hat{\mathbf{U}}|\mathbf{U}),$$

where $H(\hat{\mathbf{U}})$ is the entropy of $\hat{\mathbf{U}}$, $H(\hat{\mathbf{U}}|\mathbf{U})$ is the conditional entropy of $\hat{\mathbf{U}}$ given $\mathbf{U}$, and $I(\mathbf{U};\hat{\mathbf{U}})$ is the mutual information between $\mathbf{U}$ and $\hat{\mathbf{U}}$. Since the encoder and decoder are deterministic, invertible functions, the capacity of the system reduces in the usual way to

$$C = \max_{p(\mathbf{X})} I(\mathbf{X};\mathbf{Z}) = \max_{p(\mathbf{X})} H(\mathbf{Z}) - H(\mathbf{Z}|\mathbf{X}).$$

The channel $\mathbf{X} \to \mathbf{Z}$ is an M-ary symmetric channel (repeated n times), whose capacity depends on the probability of correct uncoded symbol detection $p \triangleq \Pr(X_i = Z_i)$. Under the assumptions of perfect timing and negligible inter-slot interference, the $M-1$ possible incorrect decisions are equally likely, and each incorrect M-PPM symbol has probability $q = (1-p)/(M-1)$. The capacity of the M-ary symmetric channel is given by [1]

$$C \quad = \quad \log_2 M + p\log_2 p + (M-1)q\log_2 q \quad \text{bits per channel use.} \tag{1}$$

Thus, to compute the capacity we need only determine p. Note that the analysis thus far has not depended on the particular type of detector used, only that the detector operates in a memoryless fashion.

3.1.2. The probability of correct detection with an APD detector

A low noise APD enhances the detection of weak optical signals by amplifying the electrical current generated by absorbed photons. This is illustrated in Fig. 2, in which the diode symbol represents the more complicated solid state components of the APD itself, and some of the APD parameters are shown in block diagram form. Unfortunately, in addition to amplifying the signal, the APD transforms the simple Poisson distribution of absorbed photons into a much more complicated probability density function at the APD output. This pdf is known [3, 13], but extremely complex to evaluate numerically. This Conradi-McIntyre distribution has been accurately approximated in a simpler formulation by Webb [20]. In particular, the probability that m secondary electrons are emitted from the APD in response to the absorption of, on average, $\bar{n}$ primary photons in a slot, is approximately

$$\Pr_w(m|\bar{n}) = \frac{\exp\left[-\frac{(m-G\bar{n})^2}{2\bar{n}G^2F\left(1+\frac{m-G\bar{n}}{\bar{n}GF/(F-1)}\right)}\right]}{\sqrt{2\pi\bar{n}G^2F}\left[1+\frac{m-G\bar{n}}{\bar{n}GF/(F-1)}\right]^{3/2}}, \tag{2}$$

where G is the average APD gain, F is the excess noise factor given by

$$F = k_{eff}G + \left(2-\frac{1}{G}\right)(1-k_{eff}),$$

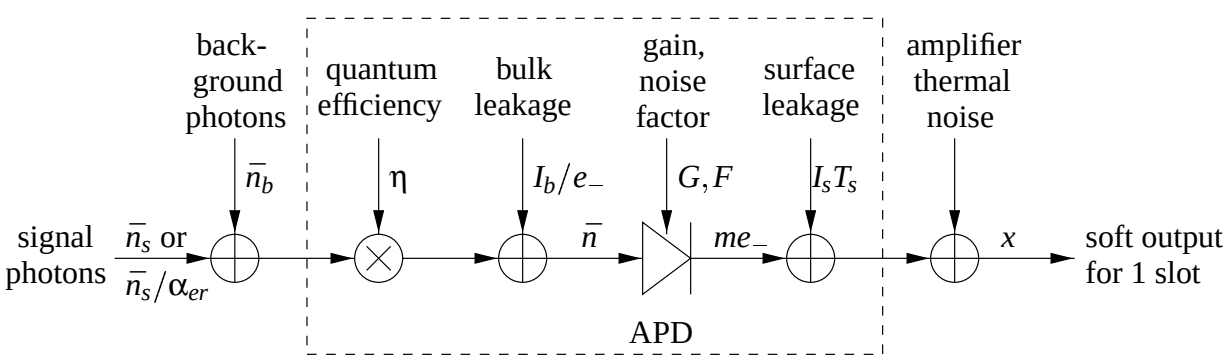

Figure 2. The soft APD demodulator.

and k_{eff} is the ionization ratio. For values of m close to its mean $G\bar{n}$, Eq. (2) can be approximated by a Gaussian pdf; however, $\mathrm{Pr}_w(m|\bar{n})$ departs greatly from a Gaussian pdf at both tails, which form the main contribution to error events in decoders [4].

The detector output x is the sum of the charge due to the approximately Webb-distributed secondary electron emissions, a contribution from the APD surface leakage current, and Gaussian distributed amplifier thermal noise, as shown in Fig. 2. Because of the thermal noise, the slot statistic x is not necessarily an integer, and may even be negative. The pdf of the sum charge is given by the convolution

$$p(x|\bar{n}) = \sum_{m=0}^{\infty} \phi(x, \mu_m, \sigma^2)\mathrm{Pr}_w(m|\bar{n}), \tag{3}$$

where $\phi(x, \mu_m, \sigma^2)$ is a Gaussian pdf with mean $\mu_m = me_- + I_s T_s$ and variance $\sigma^2 = (2e_- I_s + (4\kappa T/R))BT_s^2$, e_- is the electron charge, κ is Boltzmann's constant, T is the noise temperature, B is the single-sided noise bandwidth, and I_s is the APD surface leakage current. Note that $\mathrm{Pr}_w(m|\bar{n})$ and $p(x|\bar{n})$ are conditioned on the mean number of photons effectively *absorbed* by the detector, not *incident* the detector. The relationship between incident and absorbed photons is governed by the quantum efficiency η of the detector, as shown in Fig. 2.

The average number of absorbed photons $\bar{n}$ depends on whether the slot contains the signal. In a signaling slot, $\bar{n} = \eta\bar{n}_s + \eta\bar{n}_b + I_b/e_-$; in a nonsignaling slot, $\bar{n} = \frac{\eta\bar{n}_s}{\alpha_{er}} + \eta\bar{n}_b + I_b/e_-$. The I_b/e_- term represents the additional effective absorbed photons resulting from the APD bulk leakage current. The $\eta\bar{n}_s/\alpha_{er}$ term represents the photons absorbed when the laser is not sending a pulse. For practical purposes, the extinction ratio α_{er} is often inconsequential, being as high or higher than 10^6.

The probability of correct detection p is given by

$$p = \int_{-\infty}^{\infty} p(x|\eta\bar{n}_s + \eta\bar{n}_b + I_b/e_-) \left[\int_{-\infty}^{x} p(y|\eta\bar{n}_b + \eta\bar{n}_s/\alpha_{er} + I_b/e_-)dy\right]^{M-1} dx, \tag{4}$$

where $p(x|\bar{n})$ is the conditional pdf of the detector slot statistic given that an average of $\bar{n}$ photons are absorbed by the detector, using Eq. (3). By plugging Eq. (4) into Eq. (1), the capacity is determined. In cases where Eq .(4) is too cumbersome to numerically evaluate we may use a simpler expression as a bound and approximation. Using Jensen's inequality, p can be bounded by [18]

$$p \geq \left[1 - \int_{-\infty}^{\infty} p(x|\eta\bar{n}_s + \eta\bar{n}_b + I_b/e_-) \int_{x}^{\infty} p(y|\eta\bar{n}_b + \eta\bar{n}_s/\alpha_{er} + I_b/e_-)dydx\right]^{M-1}, \tag{5}$$

which will give a lower bound on capacity when plugged into Eq. (1). This bound is always tighter than the union bound [8], which implies that as the probability of error gets small, the ratio of the bound to the true value tends to one.

3.2. Implications of the converse of Shannon's capacity theorem

The converse of Shannon's channel coding theorem applied to the communications system in Fig. 1 implies that any error correcting code with code rate R_c information bits per transmitted bit satisfies

$$R_c(\log_2 M)(1 - \mathcal{H}_b(P_b)) \leq C(M, \bar{n}_s, \bar{n}_b, T_s, \text{detector}) \quad \text{bits per channel use}, \tag{6}$$

where $\mathcal{H}_b(x) \triangleq -x\log_2 x - (1-x)\log_2(1-x)$ is the binary entropy function, and where P_b is the coded bit error rate. Here, $R_c \log_2 M$ is the rate in bits per channel use. Note that capacity is expressed in bits per channel use, which removes its dependence on T_d. We may rewrite Eq. (6) as

$$P_b \geq \mathcal{H}_b^{-1}\left[1 - \frac{C(M, \bar{n}_s, \bar{n}_b, T_s, \text{detector})}{R_c \log_2 M}\right]. \tag{7}$$

For a given code rate R_c and fixed $(M, \bar{n}_s, \bar{n}_b, T_s, \text{detector})$, Eq. (7) gives the minimum BER P_b that any rate R_c code can achieve on the channel. Alternatively, we may write

$$R_c \leq \frac{C(M, \bar{n}_s, \bar{n}_b, T_s, \text{detector})}{(\log_2 M)(1 - \mathcal{H}_b(P_b))}. \tag{8}$$

For a given desired error rate, say $P_b = 10^{-6}$, Eq. (8) gives an upper bound on the code rate, i.e., the percentage of the transmission bits that carry information. Since the data rate $R_d = (R_c \log_2 M)/(MT_s + T_d)$ this translates directly into a bound on the data rate as well,

$$R_d \leq \frac{C(M, \bar{n}_s, \bar{n}_b, T_s, \text{detector})}{(MT_s + T_d)(1 - \mathcal{H}_b(P_b))} \quad \text{bits/sec.} \tag{9}$$

4. NUMERICAL CAPACITY RESULTS

All numerical evaluations were carried out on a 333MHz Pentium II using programs written in C and Perl. We used parameters from a 1064nm pulsed Q-switched Nd:YAG laser having slot width $T_s = 31.25$ ns, required dead time $T_d = 432000$ ns, and modulation extinction ratio $\alpha_{er} = 10^6$. This laser was chosen based on its proposed use for X2000 2nd delivery [15]. The EG&G SLiK APD has the following parameters: $k_{eff} = 0.007$, $T = 300°$K, $R = 179700\Omega$, $B = \frac{1}{2T_s}$ Hz., $I_b = 4 \times 10^{-14}$ Amp., $I_s = 2 \times 10^{-9}$ Amp., and $\eta = 38\%$. See Appendix A for a description of these parameters, or [4] for a more detailed explanation. All numerical results reported in the paper used an optimized APD gain. We discuss this optimization in Section 4.4; the optimal gain varied from 50 to 200, depending on the background level.

4.1. Bit error rate vs. background level

We used Eq. (7) to determine the lowest bit error rate theoretically possible for PPM signaling using the Nd:YAG laser and SLiK APD. The capacity was determined by numerically evaluating Eq. (5) and plugging into Eq.s (1); substitution into (7) gives the bound on bit error rate. Fig. 3 indicates the bounds when $M = 256$, As can be seen, when operating at a BER of 10^{-6}, the use of rate 7/8 codes promises the ability to withstand background levels over 40dB stronger than an uncoded system. Rate 7/8 Reed-Solomon (RS) codes operate within 3.5dB of the limit for rate 7/8 codes. In an uncoded system with $M = 256$ we must have $\bar{n}_b \leq 0.001$ in order to achieve a BER of 10^{-6}; with a RS(255,224) code we required $\bar{n}_b \leq 7.1$; and capacity implies $\bar{n}_b \leq 16.0$. Note in Table 1 that when $M = 64$, a RS code is further from capacity than when $M = 256$.

4.2. Data rate vs. background level

Using Eq. (9), a bound on the highest data rate possible while operating at a given BER and $(M, \bar{n}_s, \bar{n}_b, T_s, T_d, \text{detector})$ was calculated. As $\bar{n}_b \to 0$, the data rate tends to the maximum dictated by M, T_s, and T_d: $\log_2 M/(MT_s + T_d)$. Fig. 4 shows the maximum attainable data rate for a various M and a range of n_b, and with fixed $\bar{n}_s$, T_s, T_d, and detector. Also shown is the RS coding performance when $M = 256$.

4.3. Optimization of PPM order

Fig. 4 begs the question of what PPM order optimizes the data rate. For nighttime reception in which $\bar{n}_b \ll 1$, the optimal PPM order is near $M = 2048$. This closely follows the discussion in Section 2.2.2 regarding the errorless channel. For daytime

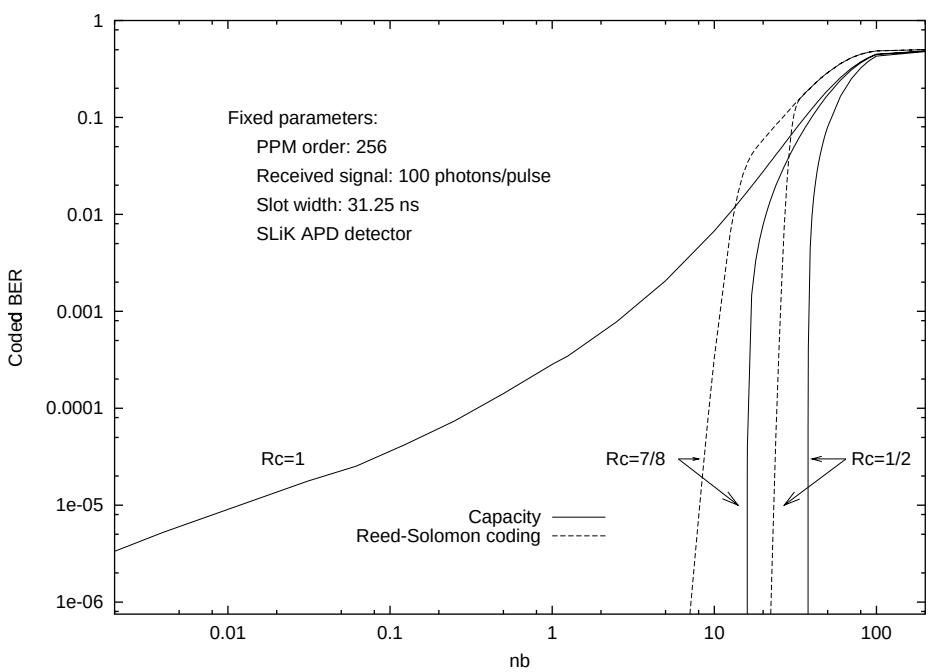

Figure 3. Comparison of RS performance to Shannon limit. Parameters: $M = 256$, $\bar{n}_s = 100$, $T_s = 31.25$ns, and the SLiK APD detector. (T_d is an irrelevant parameter.)

Table 1. Maximum background light that can be handled while operating with a coded BER of 10^{-6}. The table indicates that codes operating at the Shannon limit can withstand 2.3 to 7.6dB higher levels of background light, compared to RS codes. Parameters: $M = 256, 64, 2$, $R_c = 7/8$ or $1/2$, $\bar{n}_s = 100, T_s = 31.25$ ns, SLiK detector.

M	R_c	$\bar{n}_b$, Maximum	$\bar{n}_b$, RS coding	Difference (dB)
256	7/8	16.0	7.1	3.5
64	7/8	29.3	5.1	7.6
2	7/8	115	-	-
256	1/2	37.8	22.5	2.3
64	1/2	69.9	30.5	3.6
2	1/2	475	-	-

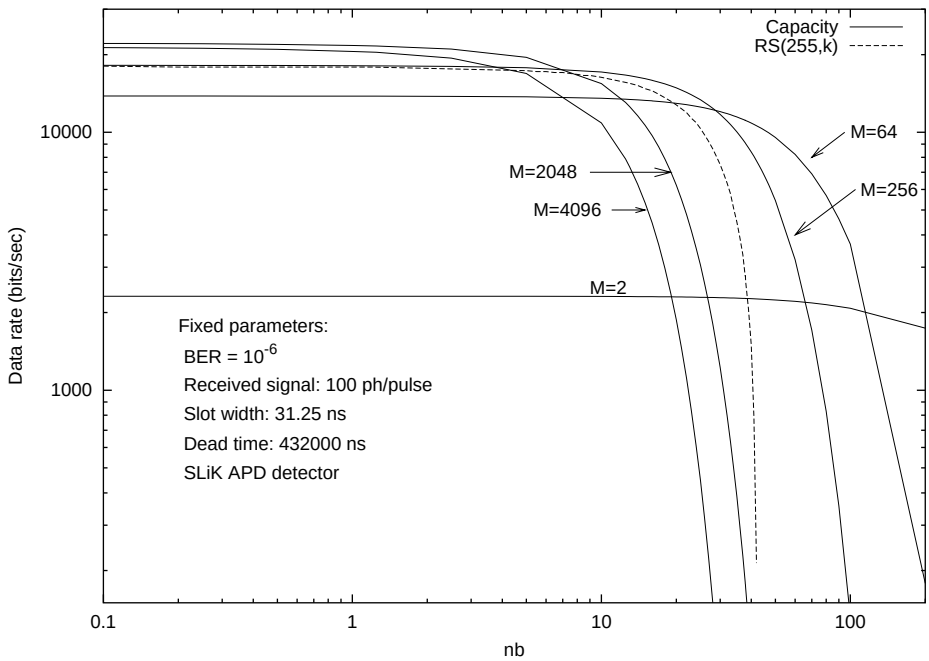

Figure 4. Capacity of M-PPM on an optical channel, with $M \in \{2, 64, 256, 2048, 4096\}$, $P_b = 10^{-6}$, $\bar{n}_s = 100$, $T_s = 31.25$ ns, $T_d = 432000$ ns, and the SLiK APD detector.

reception in which $\bar{n}_b \approx 100$, we can see from Fig. 4 that the optimal PPM order is well under 256. To be more precise, the order of PPM that maximizes capacity in bits per second can be seen directly from a plot of capacity versus M. This is shown in Fig. 5, and the optimal PPM orders for various values of $\bar{n}_b$ are summarized in Table 2.

This suggests use of a multiple PPM order communications system. During nighttime reception it should use M on the order of thousands, and during daytime reception it should use M on the order of dozens. Unoptimized PPM orders can be costly. As can be seen from Fig. 5, using $M = 2036$ during the day would be disastrous for the data rate. Using $M = 18$ at night reduces capacity by over half.

4.4. APD gain optimization

The APD gain is a parameter required to evaluate performance. For example, Eq. (2) depends on the gain. All numerical results in this paper use an optimized gain. For each value of $\bar{n}_b$, the numerical capacity or other needed quantity was computed over a range of gains, and the largest one chosen. In the interest of time, the gain was restricted to multiples of five. In all cases considered, a gain difference of five (and typically much more than five) from the optimal value made little difference in the numerical results. Shown in Fig. 6 are the optimal gain values. Optimal APD gains are also reported in [18].

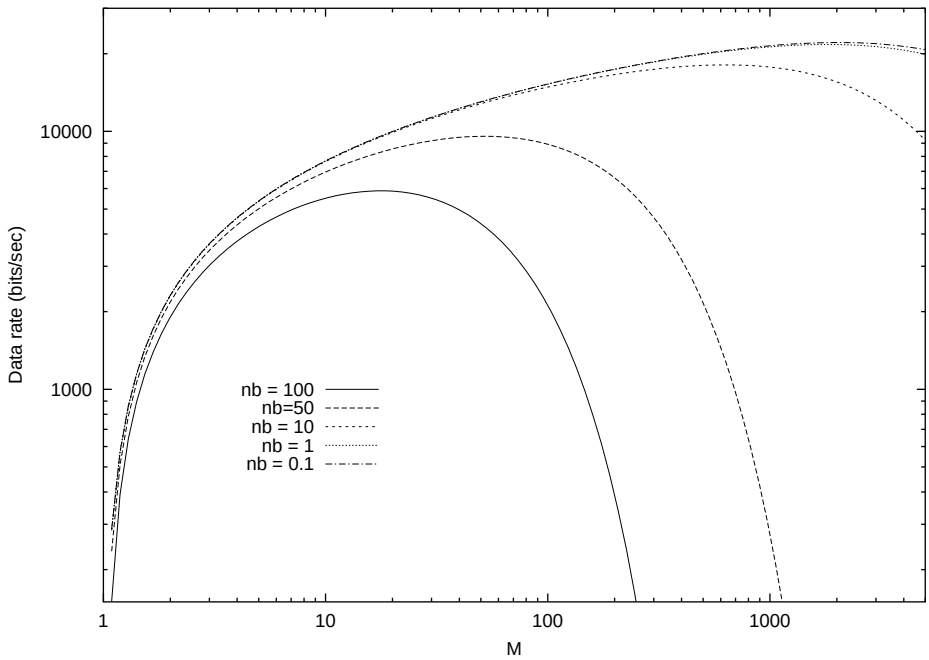

Figure 5. Capacity of M-PPM on an optical channel, with $P_b = 10^{-6}$, $\bar{n}_s = 100$, $\bar{n}_b \in \{0.1, 1, 10, 50, 100\}$, $T_s = 31.25$ ns, $T_d = 432000$ ns, and the SLiK APD detector.

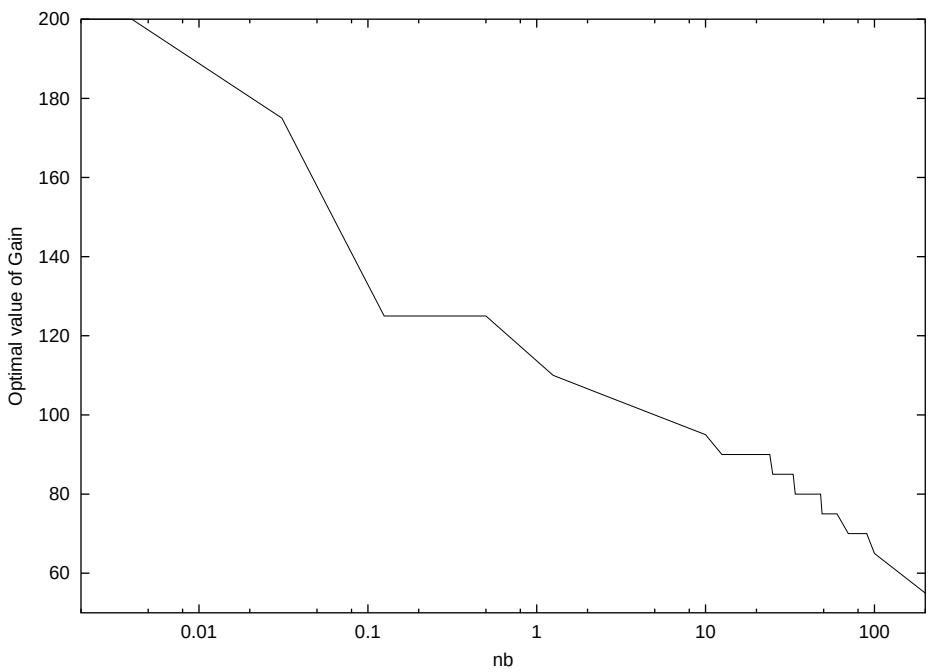

Figure 6. Optimal gain, as a function of $\bar{n}_b$, for $\bar{n}_s = 100$, $T_s = 31.25$ ns, $T_d = 432000$ ns, and the SLiK APD detector.

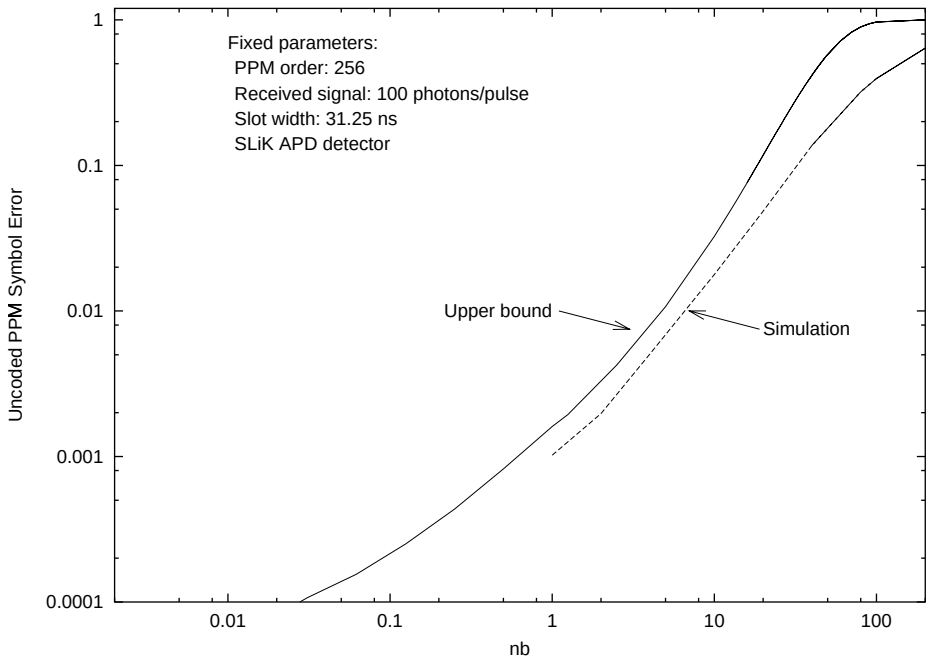

Figure 7. Probability of uncoded 256-PPM symbol error on an optical channel with $\bar{n}_s = 100$, $T_s = 31.25$ns, and the SLiK APD detector.

4.5. Comparison of simulation to upper bound of uncoded APD-detected PPM

Most numerical results in this paper required the determining the probability of uncoded PPM symbol detection error. Two approaches were taken– simulation and bounding. Using the method given in [4] to simulate the statistical properties of the APD, a channel was simulated for 100,000 256-PPM symbols. The probability of uncoded symbol error is shown in Fig. 7, and is compared to the upper bound used in Eq. (5) used to derive the remainder of the numerical results in the paper. Since the upper bound is tighter than the union bound, it necessarily converges to the true value. We see this happening, if slowly, in Fig. 7.

5. CONCLUSIONS

This paper considered an X2000 2nd delivery laser and detector, representing the current technology available. Capacity was reported in terms of BER vs. background level and data rate vs. background level. Optimization of the PPM order and APD gain were also discussed.

Results indicate that for 256-PPM and rate 7/8 coding, RS codes can handle all but the last 3.5 dB of the background levels that capacity promises can be handled while operating at a BER of 10^{-6}.

Table 2. Optimal PPM orders M when $P_b = 10^{-6}$, $\bar{n}_s = 100$, $\bar{n}_b \in \{0.1, 1, 10, 50, 100\}$, $T_s = 31.25$ ns, $T_d = 432000$ ns, and the SLiK APD detector.

$\bar{n}_b$	Optimal M
0.1	2036
1	1815
10	634
50	52
100	18

The optimal value of PPM order depends greatly on the background light. For nighttime reception, the optimal PPM order was found to be $M = 2036$, while for daytime reception, $M = 18$. With mismatched PPM order, the capacity reduces by more than a factor of two, which suggests that multiple-order PPM systems should be used if feasible.

Future advances in lasers and detectors have not been considered in this paper. Evaluating capacity for these advancements would provide very useful information regarding the limits at which the optical channel can operate. This work is straightforward but as of yet undone.

The paper also gives a framework that can be used for evaluating the sensitivity of the capacity to each parameter. Holding all parameters fixed but one, it is possible to show the sensitivity of capacity to each parameter. This would provide valuable feedback to laser and detector developers and to system designers, who could then expend effort in the areas leading to the biggest system gains. For the APD, this would include a study of the affects of the quantum efficiency, thermal noise levels, dark currents, and so forth; for the lasers, this would include the repetition rate and the pulse power. Also, note that in this paper we mostly kept $\overline{n}_s$ fixed at 100 photons per pulse. It is important to know how the capacity changes for varying $\overline{n}_s$.

Also unknown is the capacity loss due to the hard PPM symbol demodulator. Removing it and providing soft slot statistics directly to the decoder would improve capacity, and a study to quantify this gain would be an important advancement in our understanding of the optical channel.

Acknowledgements: The author thanks Meera Srinivasan for providing the C program to bound the symbol error using the APD, Juan Ceniceros for providing many FOCAS link tables, Gerry Ortiz for providing X2000 2nd delivery laser and detector parameters, and Bob McEliece for helpful discussions regarding the units of capacity and optimization of the PPM order.

APPENDIX A. PARAMETERS AND NOTATION

The following is a list of parameters and notation used in this paper.

Laser and Modulator parameters		
M	256, 64, 2	PPM order
T_s	3.125×10^{-8}	Width of the PPM slot required by laser, in seconds
T_d	4.32×10^{-4}	Dead time between PPM symbols required by laser, in seconds
α_{er}	10^6	Modulation extinction ratio
Received light		
$\bar{n}_s$	100	Average number of signal photons incident on the photodetector, per pulse
$\bar{n}_b$	0.001 - 10,000	Average number of background photons incident on the photodetector, per slot
APD detector parameters		
η	38%	Quantum efficiency
k_{eff}	0.007	Ionization ratio
T	300	Noise temperature, in Kelvin
G	50-200	Gain
R	179700	Load resistance implied by transimpedance model, $5.75 \times 10^{12} \times T_s$, in Ohms
B	$\frac{1}{2T_s}$	Noise equivalent one-sided bandwidth, in Hz.
I_b	4×10^{-14}	Bulk leakage current, in Amperes
I_s	2×10^{-9}	Surface leakage current, in Amperes
Constants		
κ	1.38×10^{-23}	Boltzmann's constant, in Joules/Kelvin
e_-	1.6×10^{-19}	Electron charge, in Coulombs
Error probabilities		
p		Probability of correct uncoded PPM detection
q		Probability uncoded PPM symbol i is detected as symbol j, $j \neq i$.

REFERENCES

1. Robert B. Ash. *Information Theory*. Dover, New York, 1965.
2. Stanley A. Butman, Joseph Katz, and James R. Lesh. Bandwidth limitations on noiseless optical channel capacity. *IEEE Trans. Commun.*, COM-30(5):1262–1264, May 1982.
3. J. Conradi. The distribution of gains in uniformly multiplying avalanche photodiodes: Experimental. *IEEE Transactions on Electron Devices*, ED-19(6):713–718, June 1972.
4. Frederic M. Davidson and Xiaoli Sun. Gaussian approximation versus nearly exact performance analysis of optical communication systems with PPM signaling and APD receivers. *IEEE Trans. Commun.*, 36(11):1185–1192, November 1988.
5. Jon Hamkins. Lower bounds on the number of required photons for reliable optical communication with PPM signals. JPL IOM 331.98.9.005, November 1998.
6. Jon Hamkins. The capacity of apd-detected ppm. *TMO Progress Report*, 42(138):1–19, August 1999.
7. Jon Hamkins. More numerical capacity results for the photon counting channel. JPL IOM 331.99.1.001, January 1999.
8. Linda W. Hughes. A simple upper bound on the error probability for orthogonal signals in white noise. *IEEE Trans. Commun.*, 40(4):670, April 1992.
9. M. Jeganathan and S. Mecherle. *FOCAS 2.0: Free-space Optical Communications Analysis Software*. Optical Communications Group, Jet Propulsion Laboratory, 4800 Oak Grove Dr., Pasadena, CA 91109, May 1998.
10. Kamran Kiasaleh and Tsun-Yee Yan. T-PPM: A novel modulation scheme for optical communication systems impaired by pulsewidth inaccuracies. *TMO Progress Report*, 42–135, November 1998.
11. James R. Lesh. Capacity limit of the noiseless, energy-efficient optical PPM channel. *IEEE Trans. Commun.*, COM-31(4):546–548, April 1983.
12. Robert J. McEliece. Practical codes for photon communication. *IEEE Trans. Inform. Theory*, IT-27(4):393–398, July 1981.
13. R. J. McIntyre. The distribution of gains in uniformly multiplying avalanche photodiodes: Theory. *IEEE Transactions on Electron Devices*, ED-19(6):703–713, June 1972.

14. George Stephen Mecherle. *Maximized data rate capability for optical communication using semiconductor devices with pulse position modulation*. PhD thesis, University of Southern California, May 1986.
15. Gerry Ortiz. X2000 2nd delivery parameters. private communication, March 1999.
16. John R. Pierce, Edward C. Posner, and Eugene R. Rodemich. The capacity of the photon counting channel. *IEEE Trans. Inform. Theory*, IT-27(1):61–77, January 1981.
17. Meera Srinivasan. Receiver structure and performance for trellis-coded pulse position modulation in optical communication systems. *TMO Progress Report*, 42–135, November 1998.
18. Meera Srinivasan and Victor Vilnrotter. Symbol-error probabilities for pulse-position modulation signaling with an avalanche photodiode receiver and Gaussian thermal noise. *TMO Progress Report*, 42-134:1–11, August 1998.
19. V. Vilnrotter, M. Simon, and M. Srinivasan. Maximum likelihood detection of PPM signals governed by an arbitrary point process plus additive gaussian noise. JPL Publication 98-7, April 1998.
20. P. P. Webb, R. J. McIntyre, and J. Conradi. Properties of avalanche photodiodes. *RCA Review*, 35:234–278, June 1974.